The Extraordinary Deaths of Ordinary Stars: Binarity and the AGB-to-PN Transformation

Raghvendra Sahai

Jet Propulsion Laboratory, Caliornia Institute of Technology

Collaborators

Wouter Vlemmings (Chalmers Institute of Technology) , Carmen-Sanchez Contreras (CSIC-INTA), Jorge Sanz-Forcada (CSIC-INTA), Mark Morris (UCLA), Samantha Scibelli (U. Arizona), Po-Sheng Huang (ASIAA,), Lars-Åke Nyman (Joint ALMA Observatory)

Funding

NASA/ GALEX GO awards; NASA/ ADAP award

Acknowledgement Statement

Sahai' s contribution to the work described here was carried out at the Jet Propulsion Laboratory, California Institute of Technology, under a contract with NASA

(Selected) Relevant References

- AGB Stars

Hofner & Olofsson 2018 (*AAR*), Decin et al. 2021 (*ARAA*)

- Pre-Planetary Nebulae

Sahai et al. 2007 (*AJ*)

- Planetary Nebulae

Sahai, Morris & Villar 2011 (*AJ*)

- AGB to PN transformation

Balick & Frank 2002 (*ARAA*)

De Marco 2009 (*PASP*)

Asymmetric Planetary Nebulae Meetings (#s 1-8e)

Ordinary Stars (~1-8 Msun)

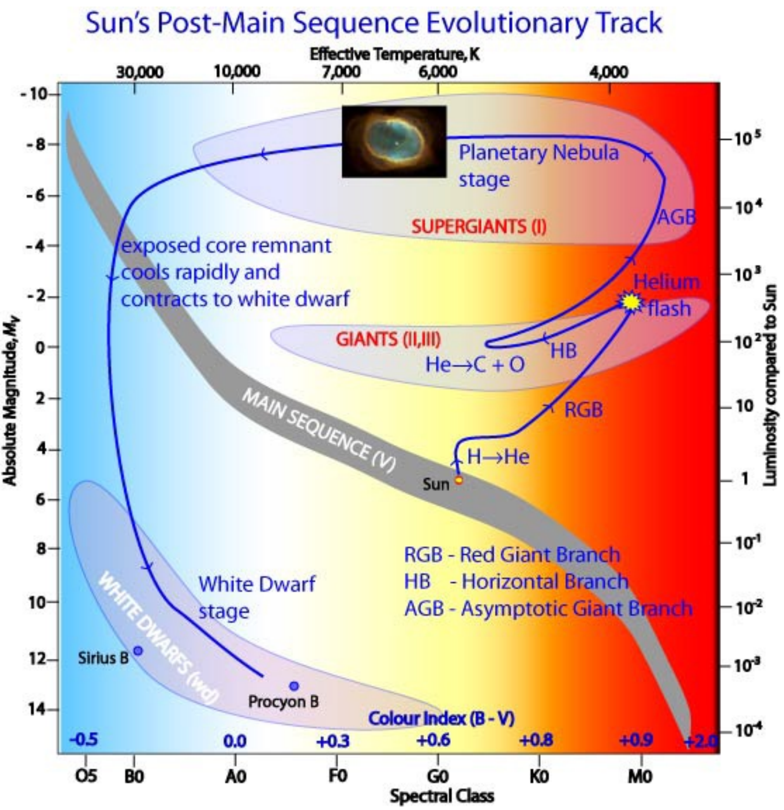

(outreach.atnf.csiro.au)

AGB evolution

- Central (C+O) degenerate core, surrounded by He & H-shells (where nuclear-burning occurs), and a very large H stellar envelope
- cool (Teff < ~3000K), very luminous (~10^4 Lsun)
- 3 chemistry types

  O-rich, C-rich, S-type (C/O <1, >1, ~1)
- **dusty, spherical expanding envelopes** at low expansion speeds (~5-20 km/s), large mass-loss rates (upto ~10^{-4} Msun/yr)

winds driven by radiation pressure on dust grains; grains drag the gas along via friction: radiative momentum L/c > ~ dM/dt x Vexp

The Extraordinary Deaths of Ordinary Stars

- stellar envelope lost due to mass-loss on the AGB, heavy mass-loss ceases
- central star begins its post-AGB evolution (towards hotter Teff) at constant L
- planetary nebula (PN) formed when Teff~30,000K (UV ionizes of molecular outflow)

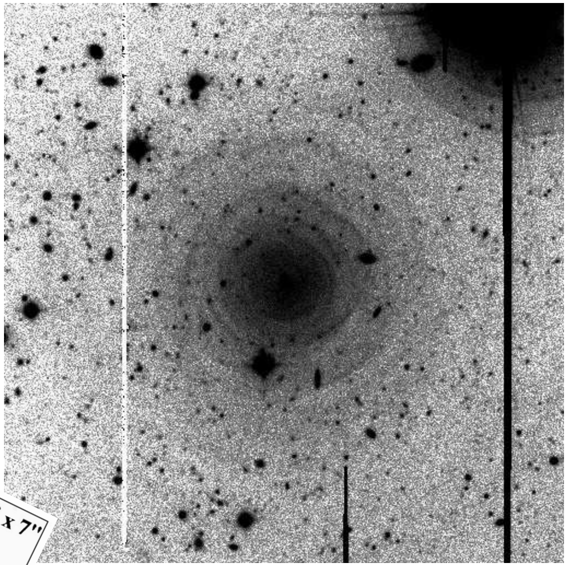

Circumstellar envelope of the **AGB star IRC+10216** illuminated by Galactic starlight (CFHT V-band: Mauron & Huggins 2000)

IRC10216 center

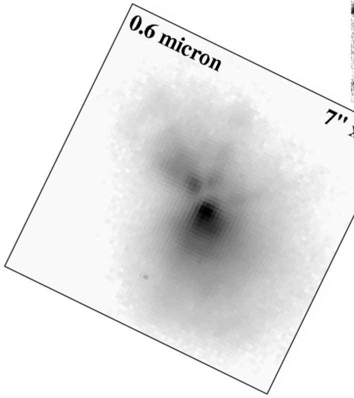

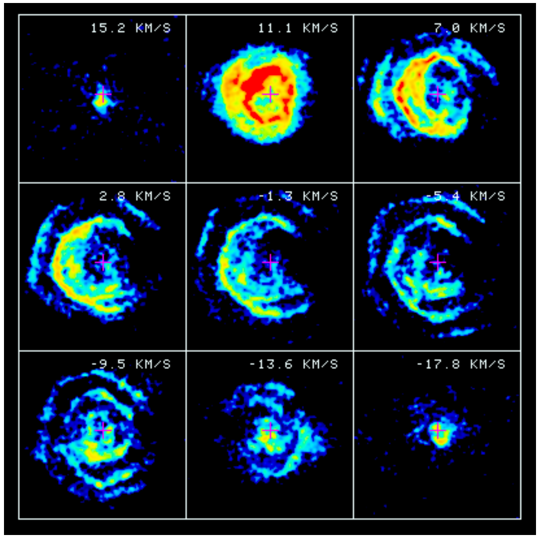

CIT-6 HC3N J=4-3 (36.39 GHz)
beam ~0.7” x 0.6”, panel size 21”
Claussen et al. (2011)

- Dramatic transformation in the morphology and outflow velocity (~100 km/s) of the mass ejecta during the intermediate evolutionary phase – the pre-planetary nebula (PPN) phase
- Process likely initiated during late-AGB phase

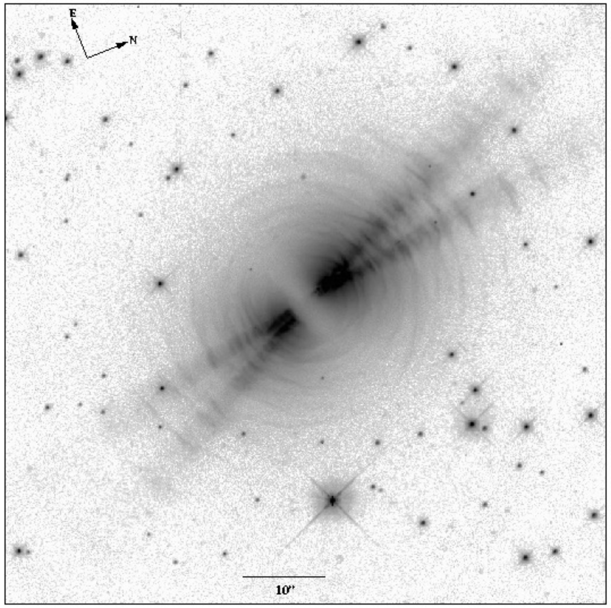

CRL2688 (C-rich PPN) *(Sahai et al. 1998a)*

The **PPN, CRL2688**, as seen in scattered light (HST, 0.6 micron)

The Progeny of AGB Stars
Pre-Planetary and Planetary Nebulae

(HST Survey) Planetary Nebulae: Class Multipolar 19% (23/119 objects)

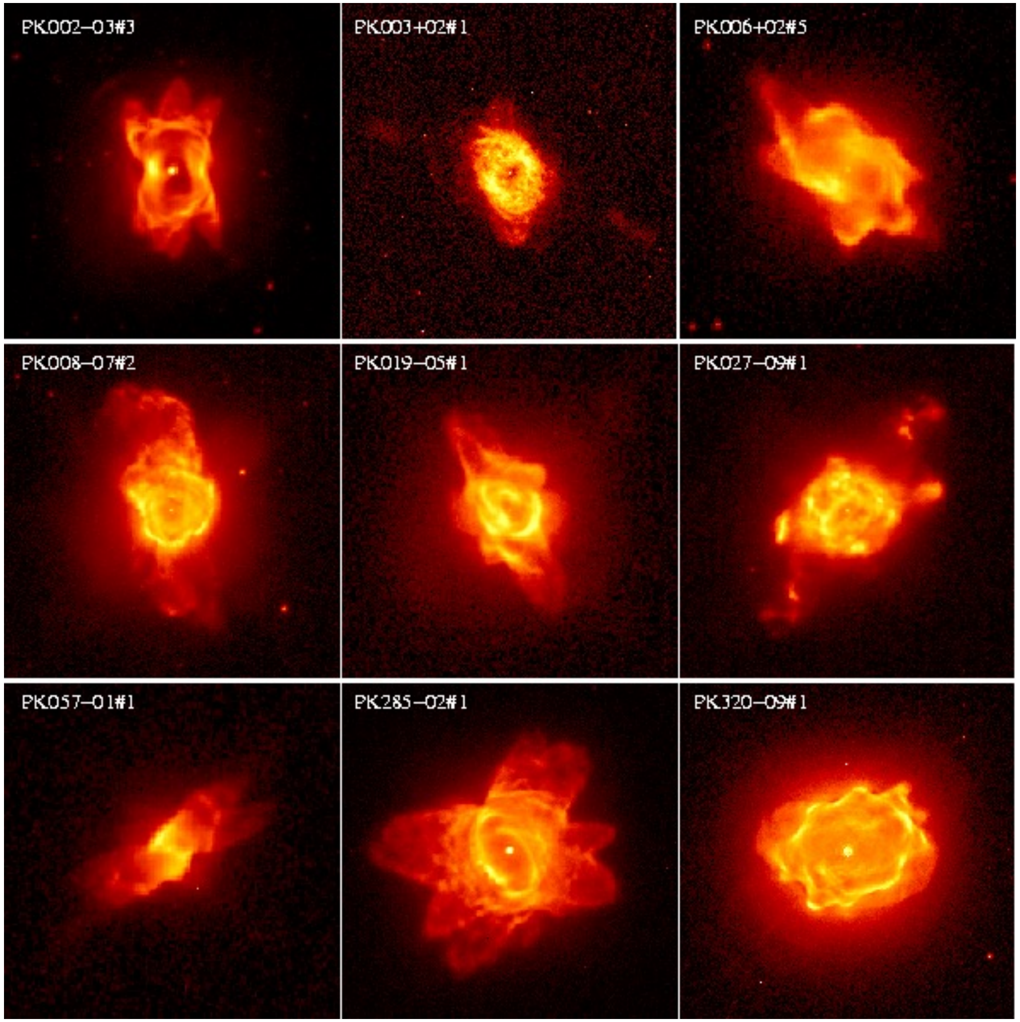

Adapted from Sahai, Morris & Villar 2011

>50% of young PNe have extreme aspherical morphologies (& point-symmetry is common) , all PPNe are aspherical
=> collimated, high-speed outflows sculpt progenitor AGB envelope from inside-out *(Sahai & Trauger 1998, Soker 1992 …)*

Binarity widely believed to be the most probable cause for producing such outflows, which must start operating during PPN or late-AGB phase

Evidence for binarity (and associated accretion-activity to make accretion disks and jets) in AGB stars?

Binarity and late-AGB & post-AGB evolution

Binarity underlying cause

Observational Indicators PN/PPNe morphologies (*e.g, Sahai et al. 2007, 2011*)

Spirals & equatorially-dense structures in AGB circumstellar envelopes, collimated outflows (e.g., *Decin+2020*)

Origins accretion-disks & jet formation (magnetic fields, rotation), common-envelope evolution, grazing-envelope evolution (e.g., *Soker2015, de Marco 2009, Chamandy+2018, Jones 2018*)

- properties of ***shaping agents: collimated fast outflows*** (~few x 100 km/s)
- properties of ***equatorially-dense structures*** (~1000 AU and **accretion-disks** (~1 AU), and their relationship (if any)
- properties of magnetic fields
- 2 (observational) subclasses of post-AGB objects? PPNe (*morphologies like young PNe*) and disk-prominent post-AGBs (*radial-velocity binaries with disks & very little extended structure*)

Nascent PPNe (nPPNe) - shaping begins early!

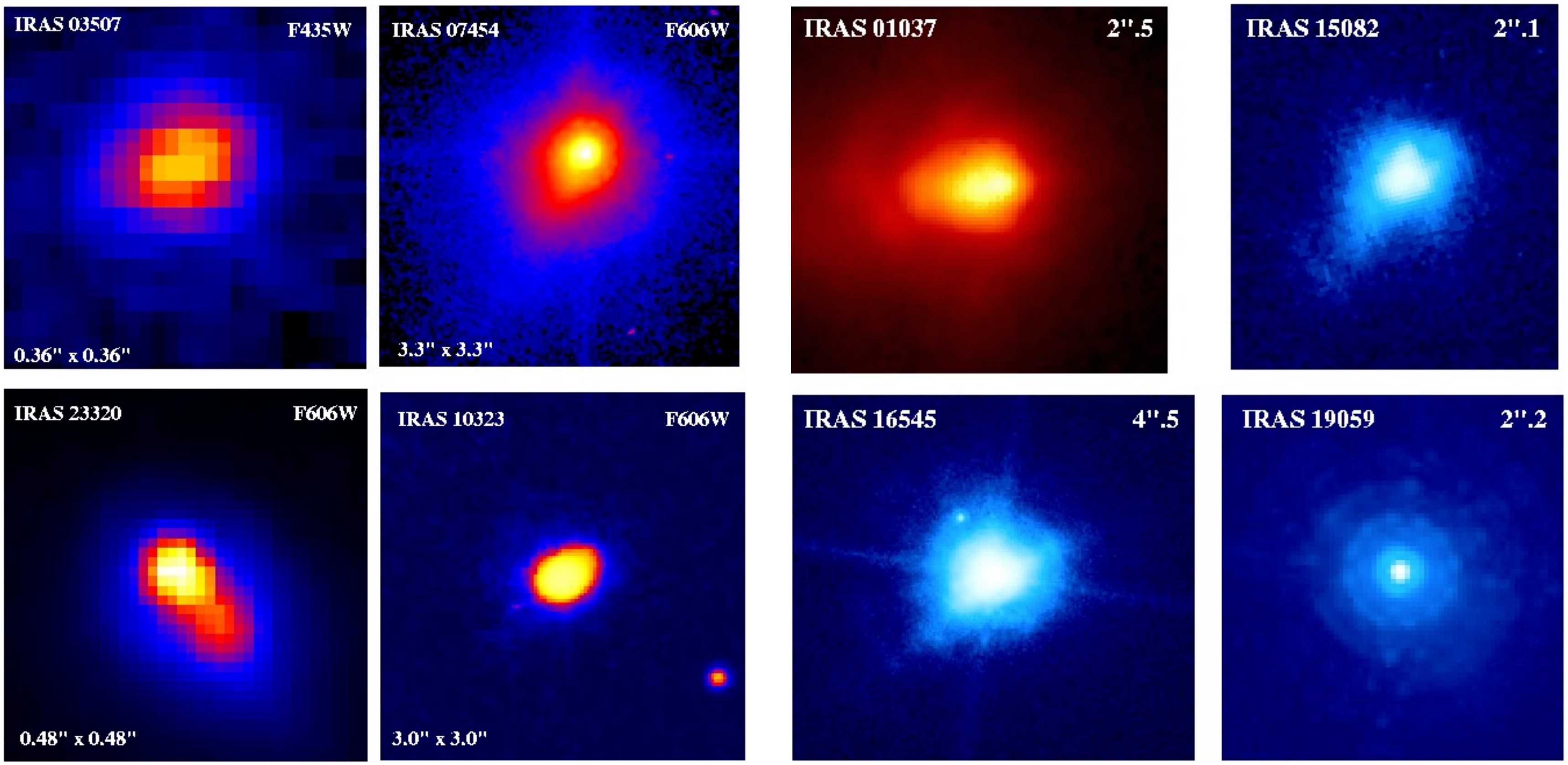

nPPN survey : 45 objects - 30% resolved, 60% show aspherical structure (*Sahai+2010*)

Compare **PPN survey** (52 objects imaged, 50% resolved, 100% of these aspherical)

Aspherical structure in the nPPNe (generally one-sided when collimated structures are seen)
=> beginning of the shaping process

V Hya: Carbon Star w/ High-Velocity Jets

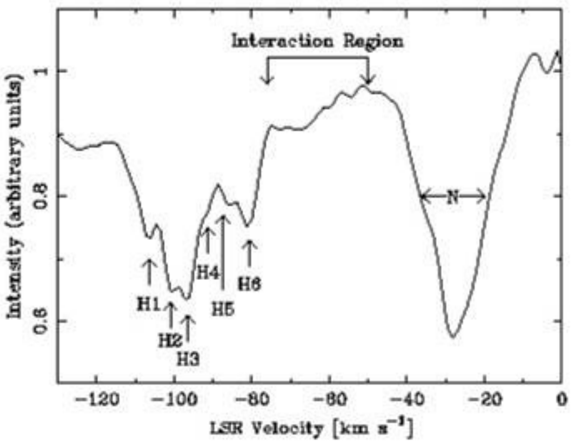

4.6 micron CO absorption *Sahai et al. (1988, 2009)*

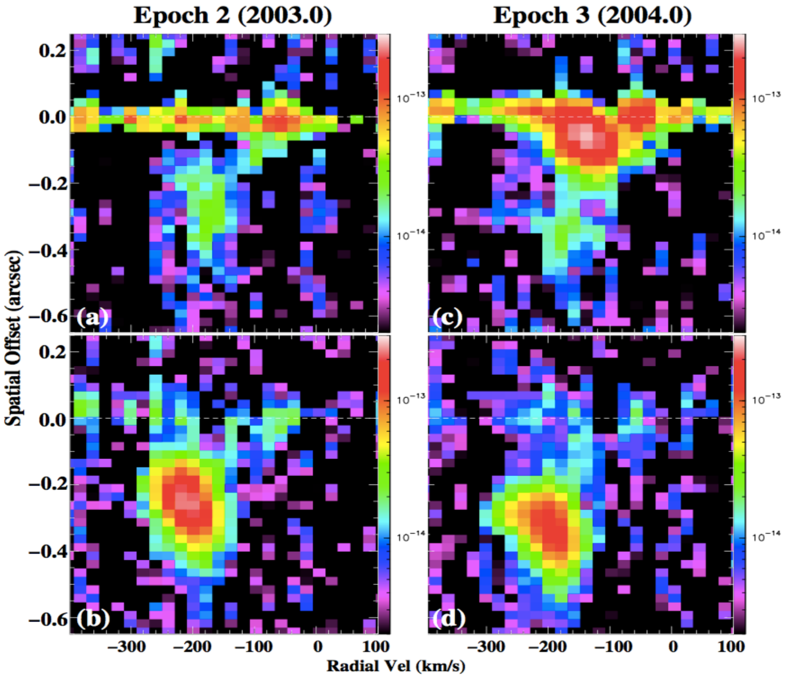

From HST/STIS data from 2002-2013, we find a 25 yr history of bullet ejection, with a projected radial velocity of about -250 km/s, measureable proper motions ~0.07 arcsec/yr

SII emission (PV plot) *Sahai et al. (2003, 2016)*

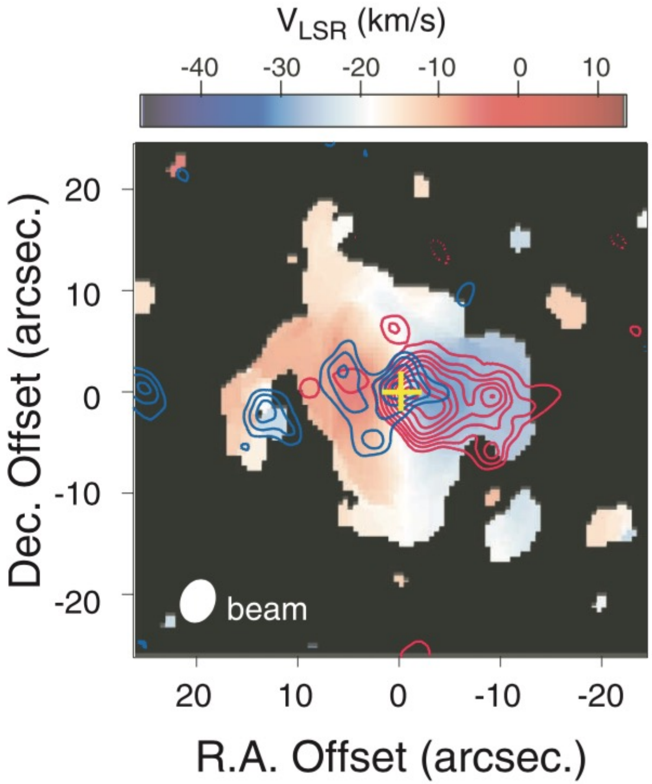

CO J = 2 – 1 map *Hirano et al. (2004)*

ALMA Cycle 5 program to observe V Hya at ~0.25 arcsec resolution

V Hya: ALMA 0.8-1.3 mm study

(*Sahai et al. 2022*)

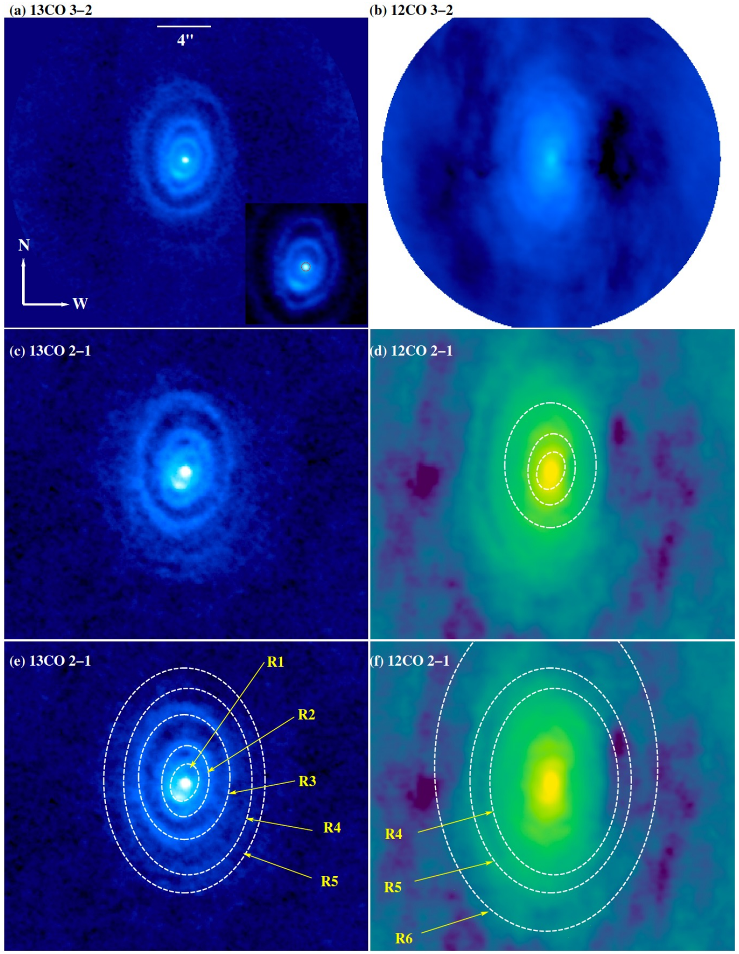

A Multi-Ring Circus!

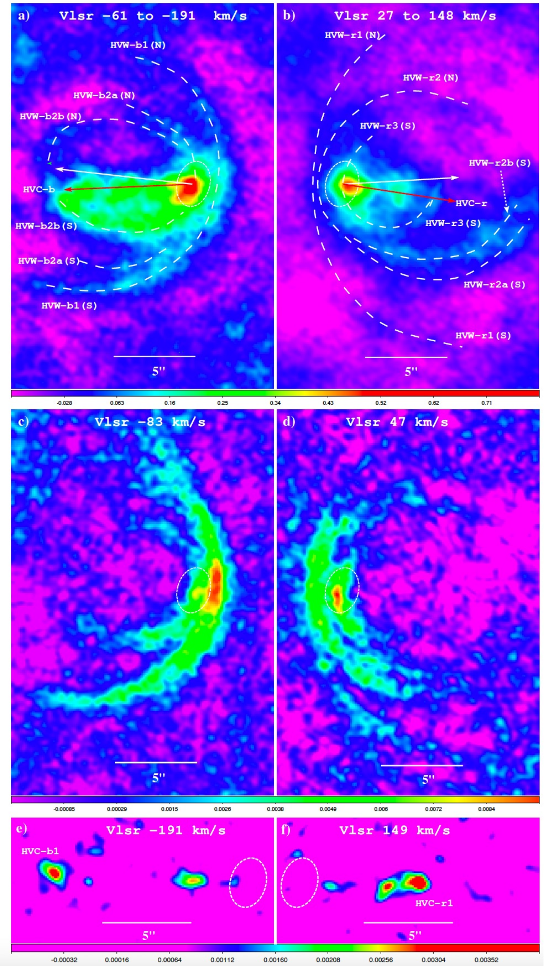

Multiple High-Velocity Outflows

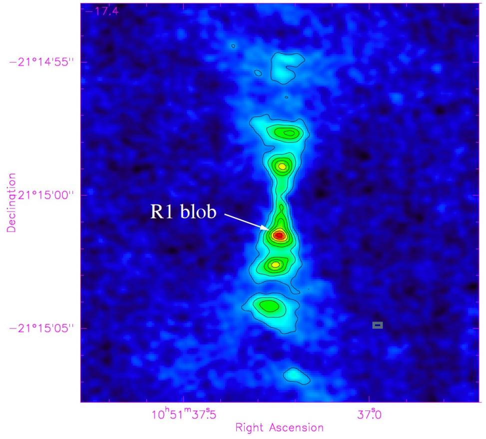

The flared central Disk Undergoing Dynamical Expansion (DUDE)

The Youngest PPNe: Water-Fountain PPNe

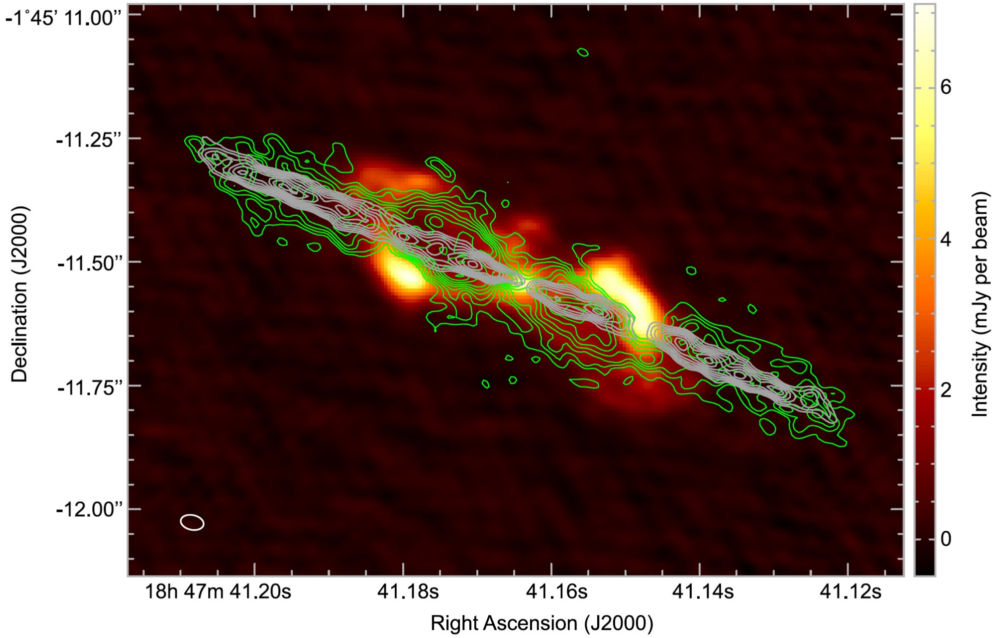

W43A: ALMA image of the 1.3 mm continuum (colorscale) and CO 2-1 line emission (contours: (green) Vexp< 75 km/s, (grey) Vexp~75-100 km/s)

Yung, Nakashima, Imai et al. 2011
Imai & Tafoya 2011
Imai, Morris & Sahai 2007

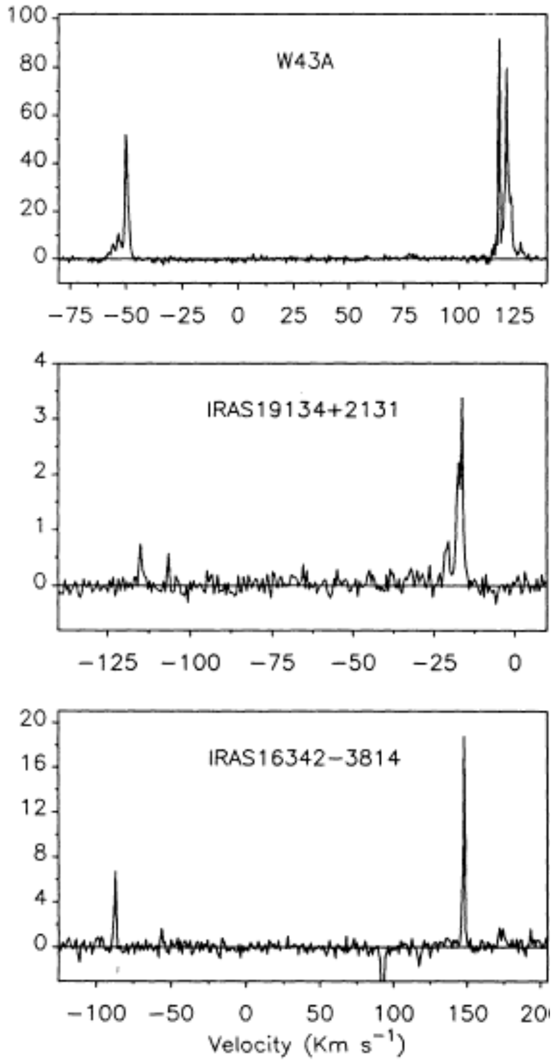

(*Likkel & Morris1988, Likkel et al. 1992*)

IRAS16342

Sahai et al 2017

^{12}CO 3-2 moment 0 map

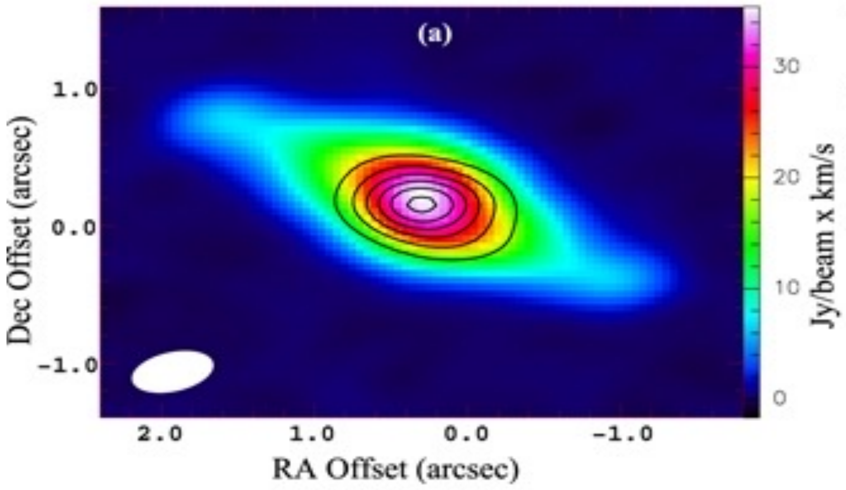

Compact bipolar outflow (+/- 260 km/s), **PA=68 deg**

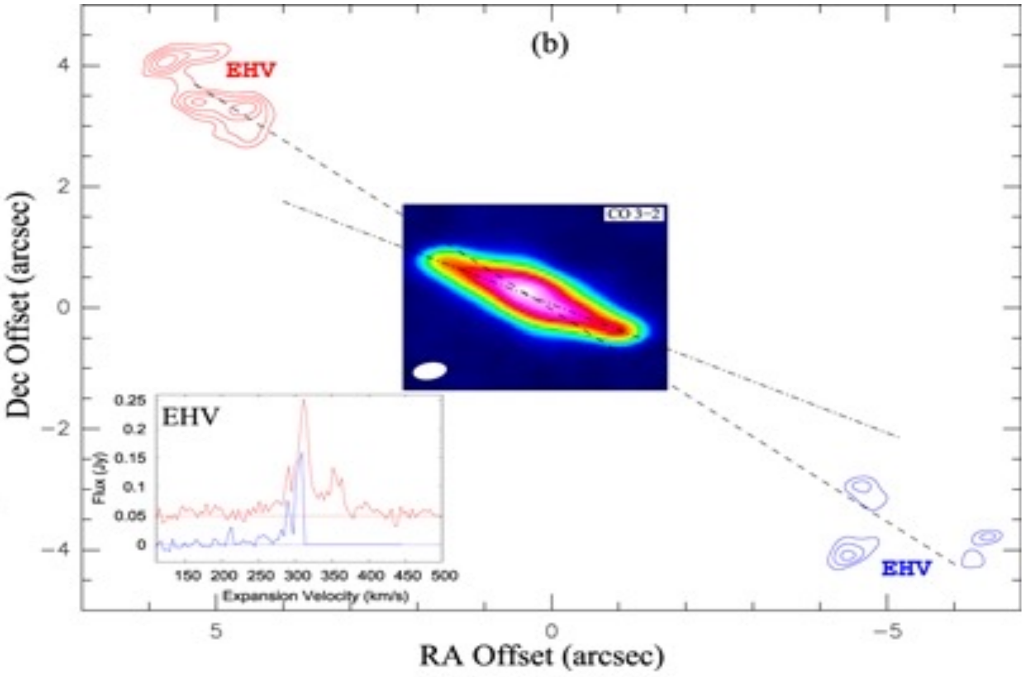

Extended bipolar outflow (+/- 300 km/s) **PA=58 deg**

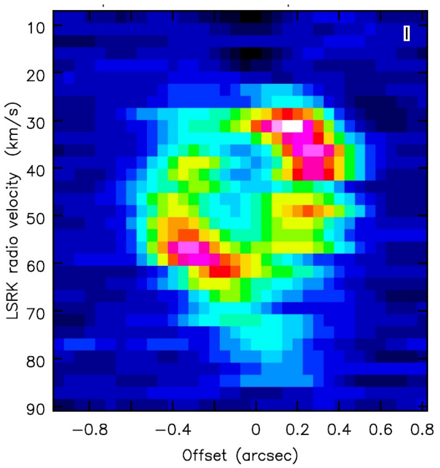

Torus/ring structure in H^{13}CN 4-3 (radius=640AU)
Generally consistent with expansion, but *tilt of PV ellipse: possible rotational component*)

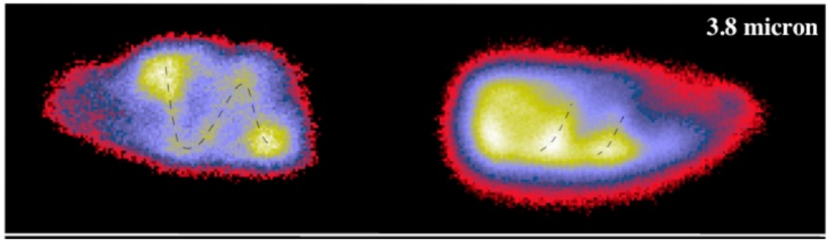

(*Sahai et al. 2005*)

Keck/AO image: corkscrew structure, signature of a precessing jet (e.g., *Cliffe et al 1995*)
Jet-beam diam. < 100 AU, jet precession P <=50 yr

IRAS16342

(*Sahai et al. 2017*)

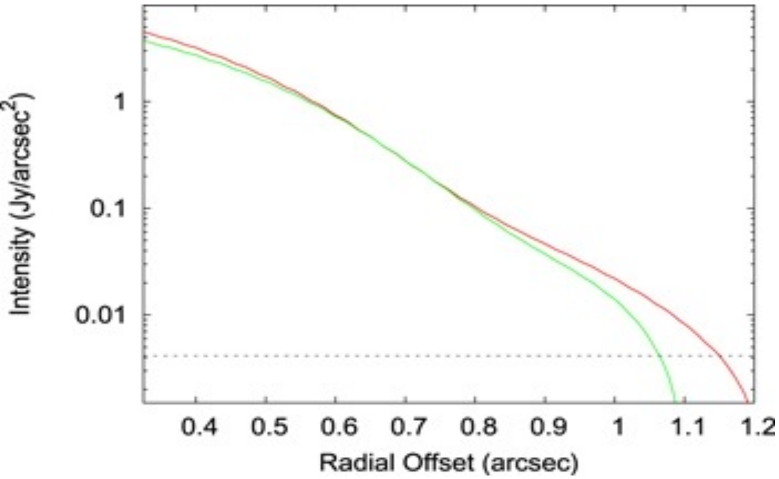

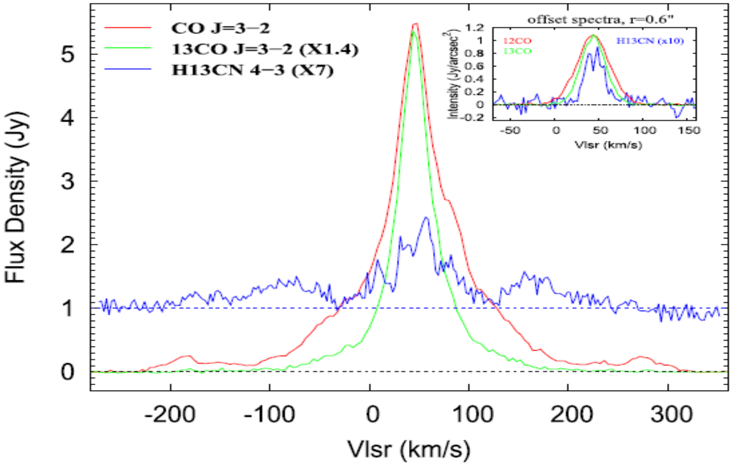

^{12}CO 3-2 and ^{13}CO 3-2 intensity (and abundance) fall very rapidly at ~1 arcsec => dM/dt (>3.5e-4 Msun/yr), increased rapidly 450 yr ago

Vexp likely increases with radius

Binary Interaction Chronology

0) Rapid, very large increase in dM/dt

1) torus formation (age ~160 yr)

2) high-speed jets: two episodes

dominant one has age ~110 yr

weaker one has age ~300 yr

(*following Blackman & Lucchini 2014*)

high momentum rate =>

high minimum accretion rate =>

NO standard Bondi–Hoyle–Lyttleton wind accretion and wind Roche-lobe

overflow (RLOF) models with white-dwarf or main-sequence companions.

YES enhanced RLOF from the primary

or accretion modes operating within common-envelope evolution

Increasing number of high angular-resolution studies are revealing the fundamental physical properties of the mass-ejecta in PPNe

(e.g., OH231.8+4.2: *Sanchez Contreras et al. 2018*, M2-9: *Castro-Carrizo et al. 2017*, IRAS19475: *Sanchez Contreras et al. 2006*)

New Evolutionary Path to the post-AGB phase
Dusty post-RGB stars

- **Boomerang Nebula, and (possibly) HD101584**
  2 examples in our Galaxy (*Sahai et al. 2013, 2017, Oloffson et al. 2019*)
- **119 dusty objects in LMC and 45 in SMC identified as post-RGBs (**spectroscopy to determine Teff, log(g)**)**

  Kamath, Wood & Van Winckel (2014, 2015)
- **Finding post-RGBs amongst dusty evolved objects in the MCs easier, because no distance ambiguity, enables reliable Luminosity determination**
- **Teff, log g, [Fe/H] similar to post-AGB, *however* much lower Luminosities (< 2500 L_sun)**
- **SEDs show evidence for *circumstellar envelopes* shells and/or disks — similar to post-AGBs**

Post-RGB Stars in the Magellanic Clouds

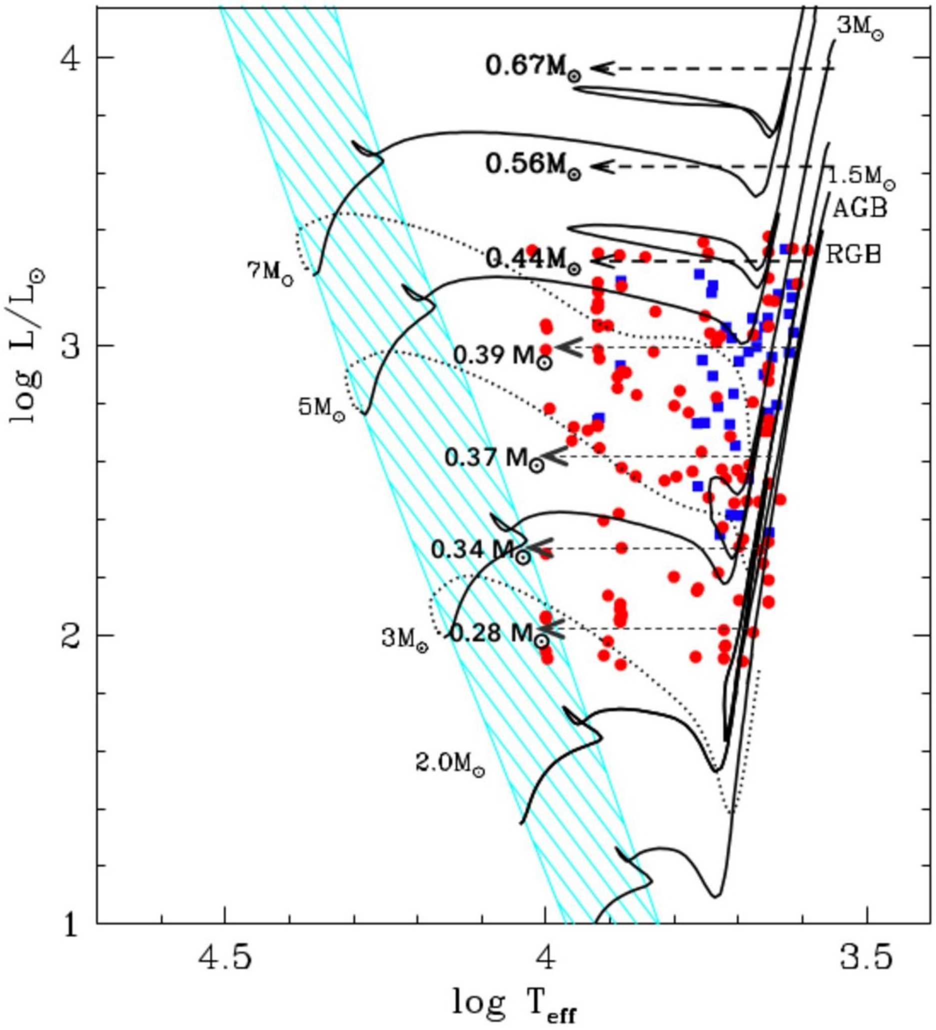

post-RGB stars in the MCs

LMC (red circles), SMC (blue squares)

- Main-sequence (MS): cyan, cross-hatched region
- Black solid lines: evolutionary tracks from MS to AGB-tip
- Black dashed arrows (*post-CEE for RGBs*):

post-RGB tracks (final mass <~0.44 Msun)

post-AGB tracks (final mass >~0.44 Msun)

Boomerang Nebula
(also the coldest object in the Universe!)

(Sahai & Nyman 1997, Sahai et al. 2013, 2017)

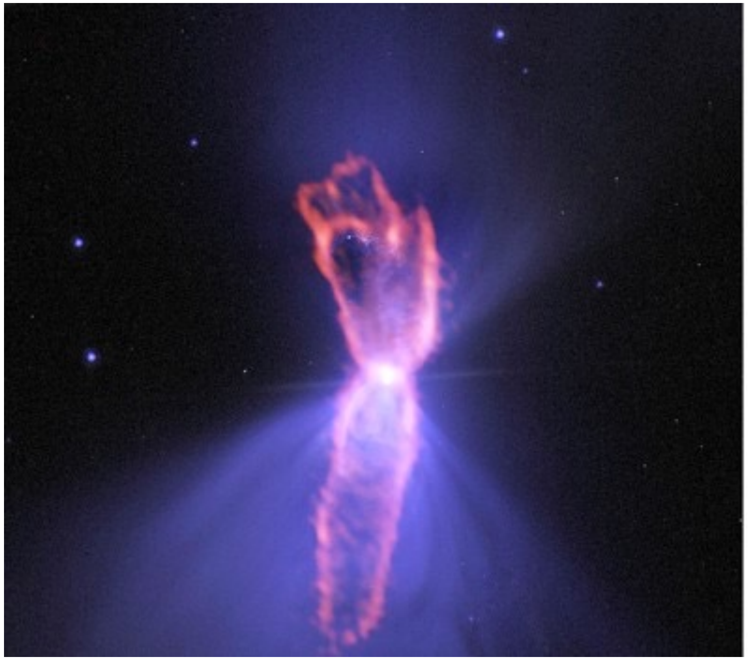

ALMA CO 2-1 (red), HST 0.6 micron (blue)

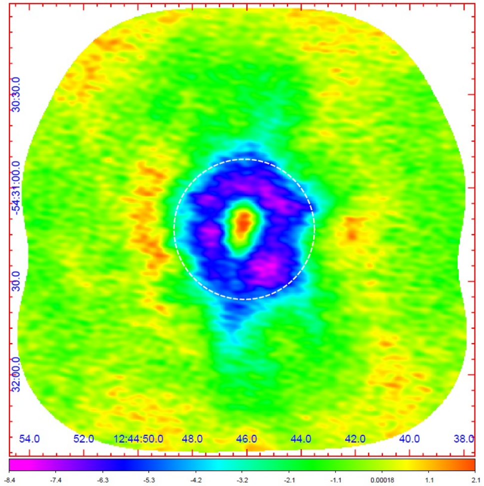

ALMA CO 1-0

Extreme Mass-Outflow Properties

- dM/dt ~1e-3 Msun/yr
- Vexp ~ 165 km/s
- envelope outer radius ~120,000 AU
- Teff ~ 6000 K
- yet L <~300 Lsun! (*hence, post-RGB*)

HD 101584

(Olofsson et al. 2017, 2019)

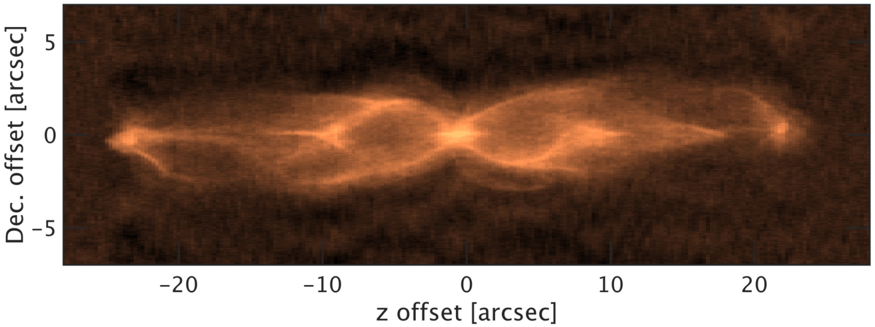

Circumstellar environment of HD 101684 as seen from the side, reconstructed from channel maps assuming Vexp ~ r

Only two examples of post-RGB objects in our Galaxy *(distance constraints adequate to set upper limit on Lum)*

Physical properties of ejecta (e.g., kinematics, morphology) very similar to those of PPNe

SED Modeling Study of pRGB sources in the LMC

Sarkar & Sahai 2022

J050257.89-665306.3

post-RGB (Kamath e al. disk) source

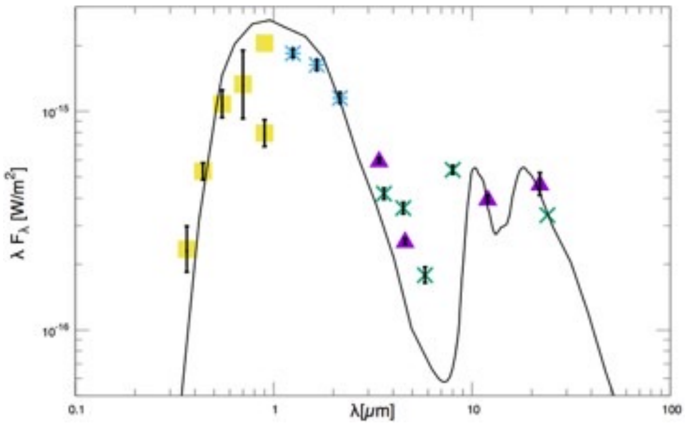

one-component model

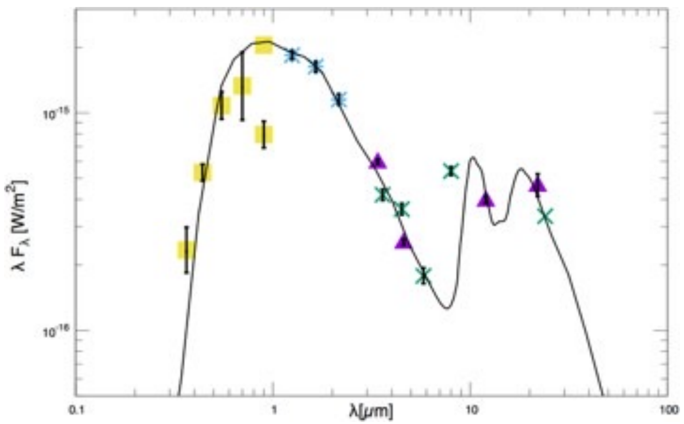

two-component model
(inner warm disk + cool outer shell)

J051920.18-722522.1

post-RGB (Kamath et al. shell) source

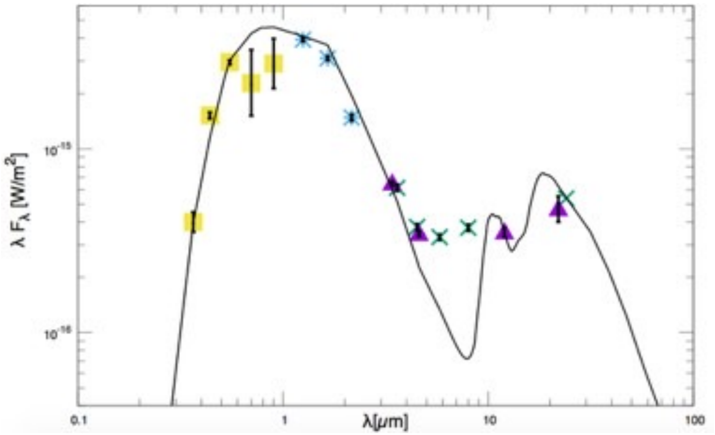

one-component model

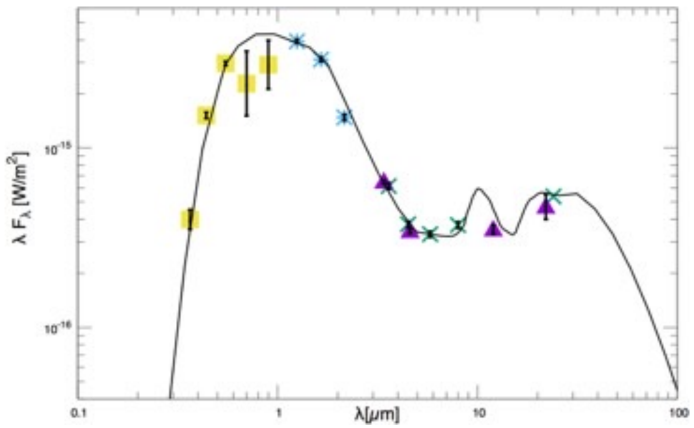

two-component model
(inner warm disk + cool outer shell)

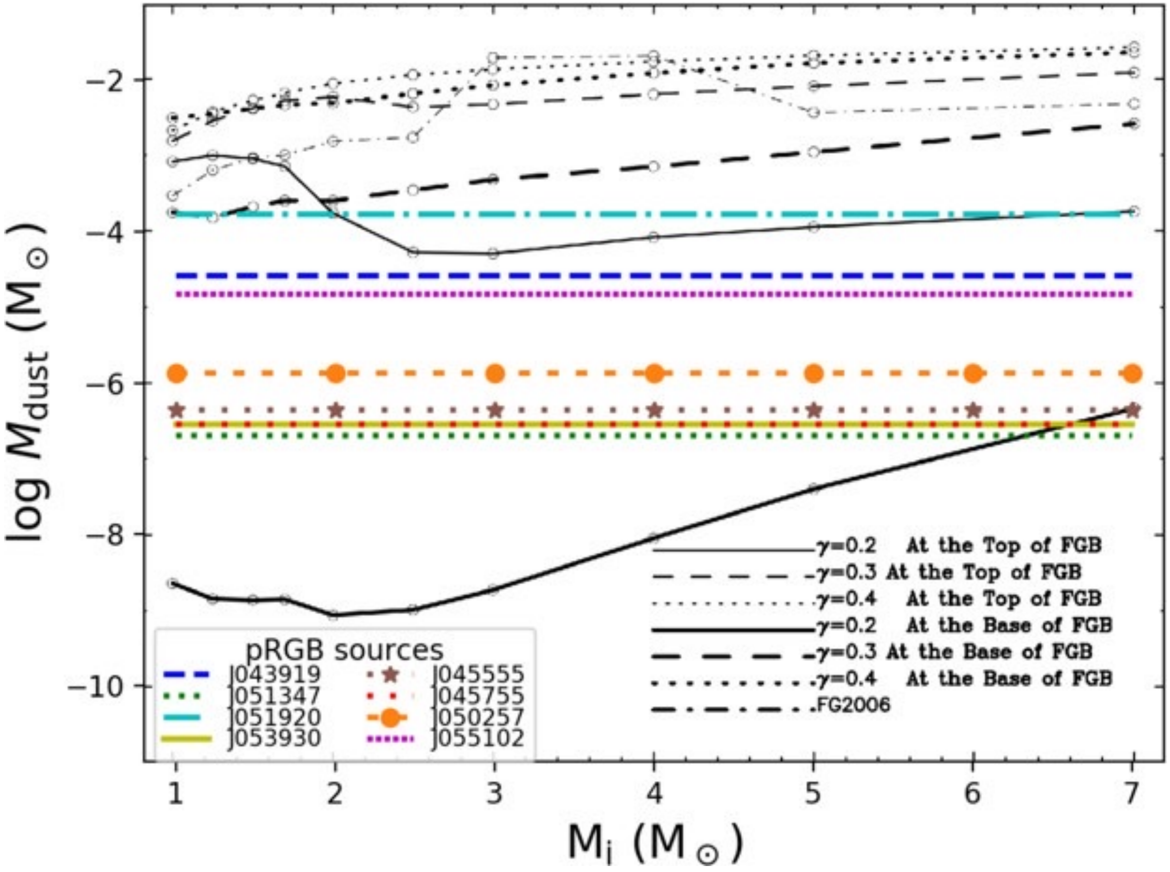

The inferred circumstellar dust mass for the post-RGB sources in this study (colored horizontal lines), overplotted on curves of dust masses in CEE systems (from Lu et al. 2013). CEE occurred most likely near or at the tip of the RGB for our sources.

Summary of important derived parameters *(Sarkar & Sahai 2021)*

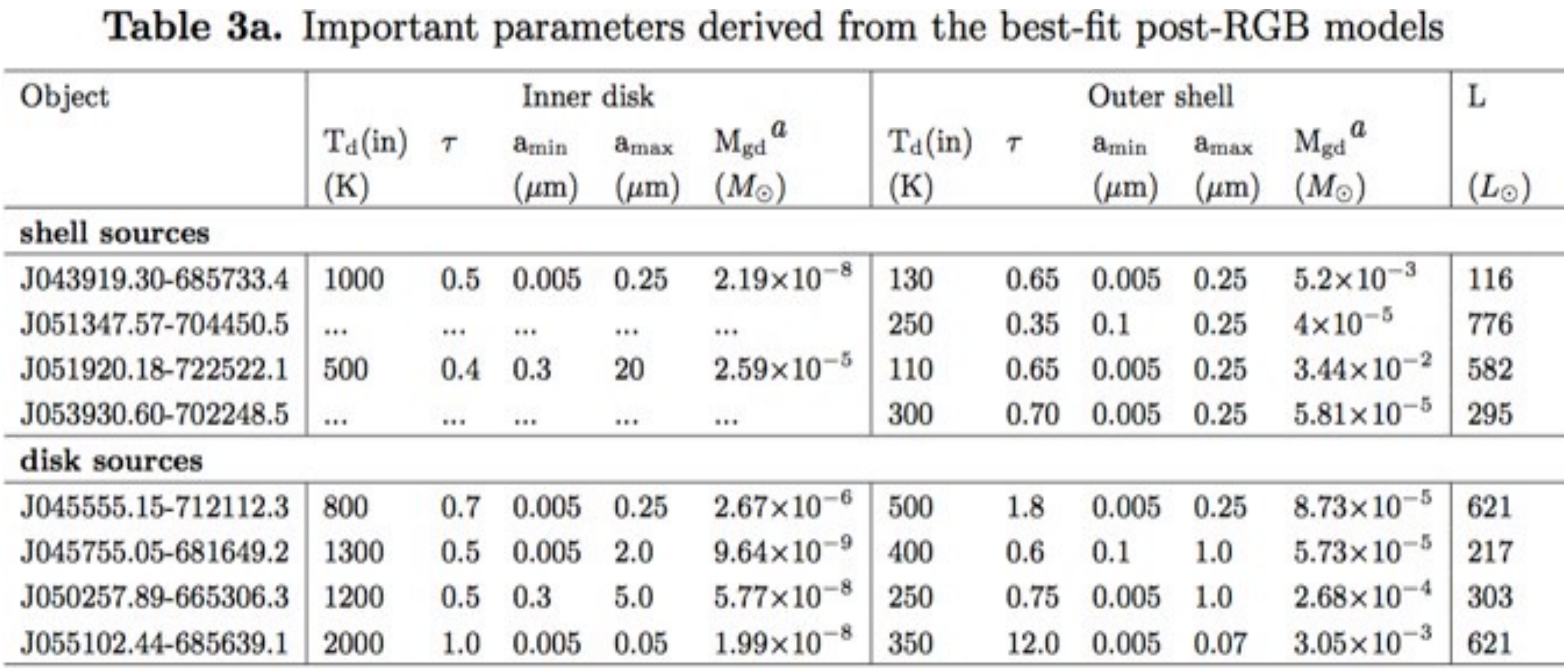

Table 3a. Important parameters derived from the best-fit post-RGB models

Object	Inner disk					Outer shell					L
	T_d(in) (K)	τ	a_{min} (μm)	a_{max} (μm)	M_{gd} [a] ($M_\odot$)	T_d(in) (K)	τ	a_{min} (μm)	a_{max} (μm)	M_{gd} [a] ($M_\odot$)	($L_\odot$)
shell sources											
J043919.30-685733.4	1000	0.5	0.005	0.25	2.19×10^{-8}	130	0.65	0.005	0.25	5.2×10^{-3}	116
J051347.57-704450.5	...	...	...	...	...	250	0.35	0.1	0.25	4×10^{-5}	776
J051920.18-722522.1	500	0.4	0.3	20	2.59×10^{-5}	110	0.65	0.005	0.25	3.44×10^{-2}	582
J053930.60-702248.5	...	...	...	...	...	300	0.70	0.005	0.25	5.81×10^{-5}	295
disk sources											
J045555.15-712112.3	800	0.7	0.005	0.25	2.67×10^{-6}	500	1.8	0.005	0.25	8.73×10^{-5}	621
J045755.05-681649.2	1300	0.5	0.005	2.0	9.64×10^{-9}	400	0.6	0.1	1.0	5.73×10^{-5}	217
J050257.89-665306.3	1200	0.5	0.3	5.0	5.77×10^{-8}	250	0.75	0.005	1.0	2.68×10^{-4}	303
J055102.44-685639.1	2000	1.0	0.005	0.05	1.99×10^{-8}	350	12.0	0.005	0.07	3.05×10^{-3}	621

(a) The total mass, derived assuming a gas-to-dust ratio of g2d=200

- **Ejected matter may be C-rich in some sources**, **e.g. post-RGB source: J055102.44-685639.1 disk: amorphous C, shell: silicates + SiC**
- **Discrepancy between model and observed SED suggests PAH emission (UV flux may not be imperative for PAH excitation (*Li & Draine 2002*)**
- **Ejected mass is VERY LOW compared to the mass that MUST BE EJECTED for star to lose its stellar envelope and proceed on post-RGB track**

Where is the Missing Mass?

2/8 post-RGB sources detected with Herschel surveys of the LMC (*Seale+2014, Meixner+2013*)

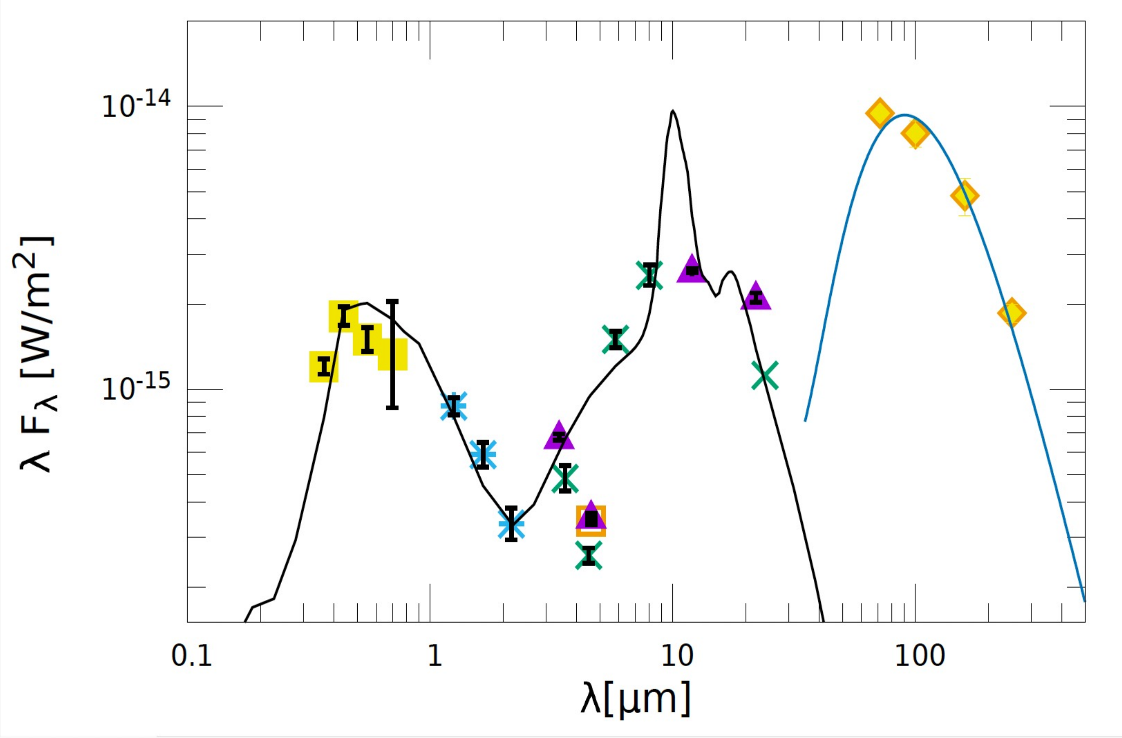

most of the ejected mass lies in cool shell

since max M(tot) for a intermediate-mass star is ~7 Msun

p < 1.0 and/or gtd < 200 and/or swept-up ISM

J045555

- Herschel photometry
- PACS 70, 100, 150 micron
- SPIRE 250 micron

reveals

cool massive shell!

- simple, one-temperature fit with dust emissivity $\kappa \sim \nu^p$, p=1

T=32 K, M(dust)=0.09 Msun

=>

M(tot) ~ 18 (g2d/200) Msun,

(g2d = gas-to-dust ratio)

Where is the Missing Mass?

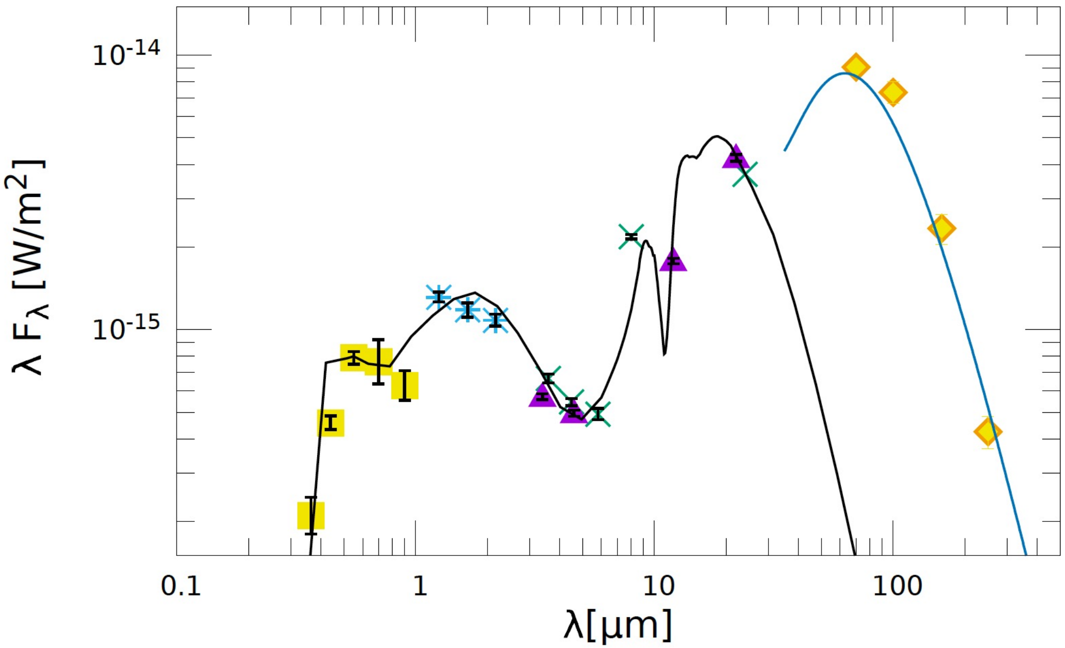

most of the ejected mass lies in cool shell

HAWC+ can detect the missing mass (e.g., S/N=5 in Bands C & D (89 & 154 micron) in integration times ~ 1 hr)

J055102

- Herschel photometry
- PACS 70, 100, 150 micron
- SPIRE 250 micron

reveals

cool massive shell!

- simple, one-temperature fit with dust emissivity $\kappa \sim \nu^p$, p=1

T=45 K, M(dust)=0.015 Msun

=>

M(tot) ~ 3 (g2d/200) Msun,

(g2d = gas-to-dust ratio)

Disk-prominent post-AGB stars

Post-AGB stars that are known (or suspected) radial-velocity binaries (radial-velocity data e.g., *Oomen+2018, van Winckel et al. 2008*)

Weak or no extended outflows (as seen in PPNe), but prominent disks

Disks inferred from from SED/spectral modelling (*de Ruyter+2005,06; Gielen+2007,09*)

Direct (interferometric) detection of disks: VLTI (*e.g., Deroo+2007, Hillen+2016*)

CO observations (*Bujarrabal+2005,2016,2017,2018*)

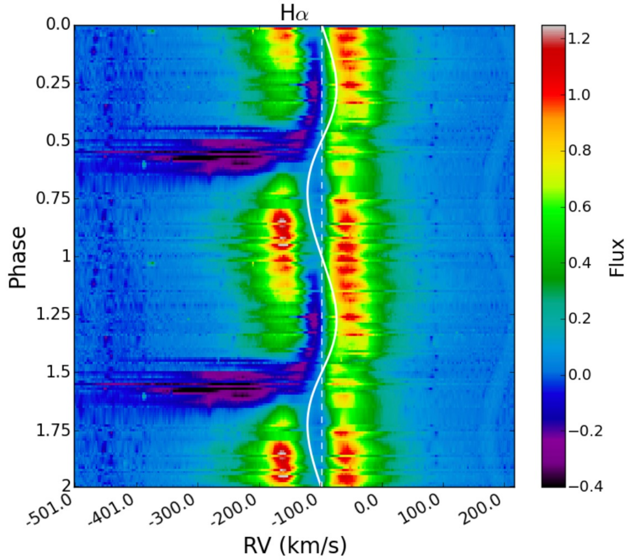

BD+46°442: Dynamic spectra of the photospheric-subtracted Ha profile as a function of orbital phase (*Bollen+2017,2020*)

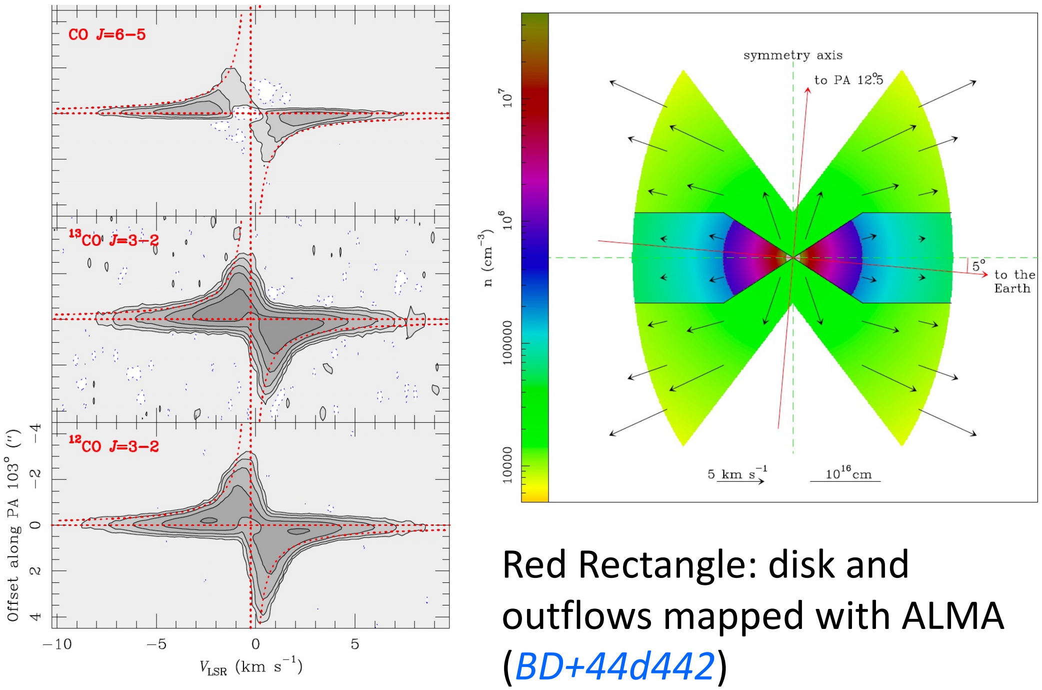

Red Rectangle: disk and outflows mapped with ALMA (*BD+44d442*)

Planetary Nebulae

Herschel study of select PNe w/ PACS, SPIRE (HerPlaNS: PI T. Ueta)

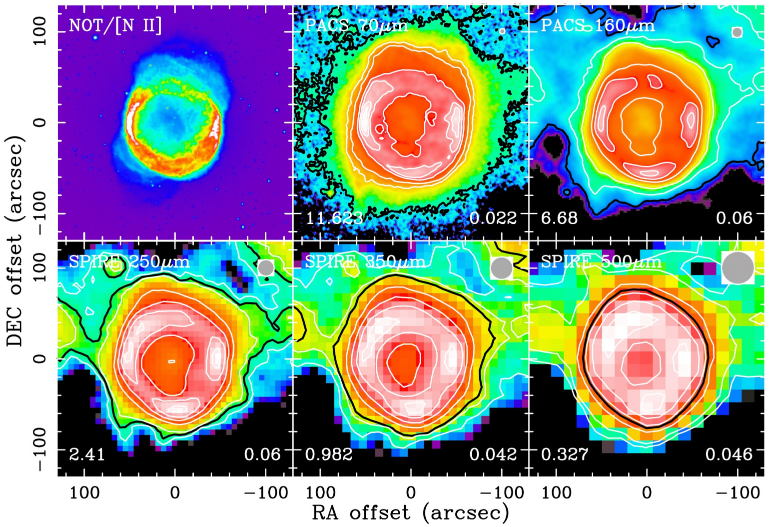

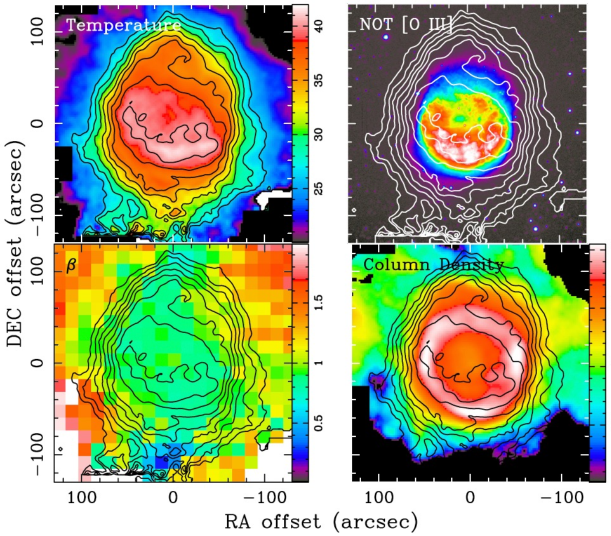

Ueta et al. (2014, 2019), Otsuka et al. (2017)

A survey of young PNe with different morphologies in the main far-IR cooling lines (e.g. [CII] 158 micron, [OI] 63 micron) needed to probe the final phase of mass-loss that lead to the formation of PNe

C+ (not CO) is better tracer of mass ejecta in young PNe (e.g., [CII] mapping of Ring Nebula, *Sahai et al. 2012*)

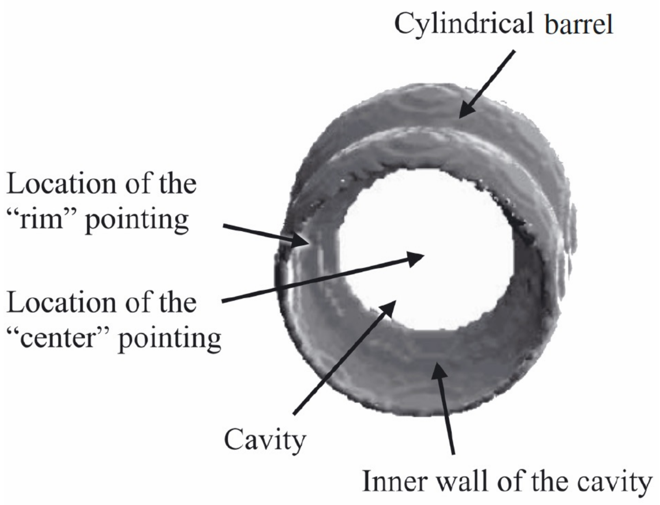

3-density-component CLOUDY model

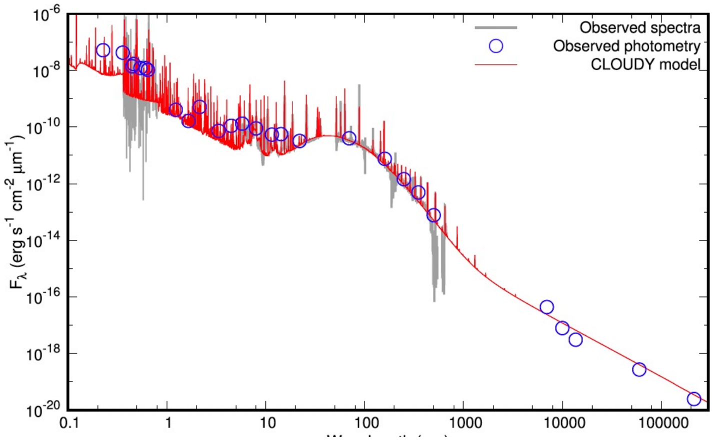

Search for Binarity in AGB Stars

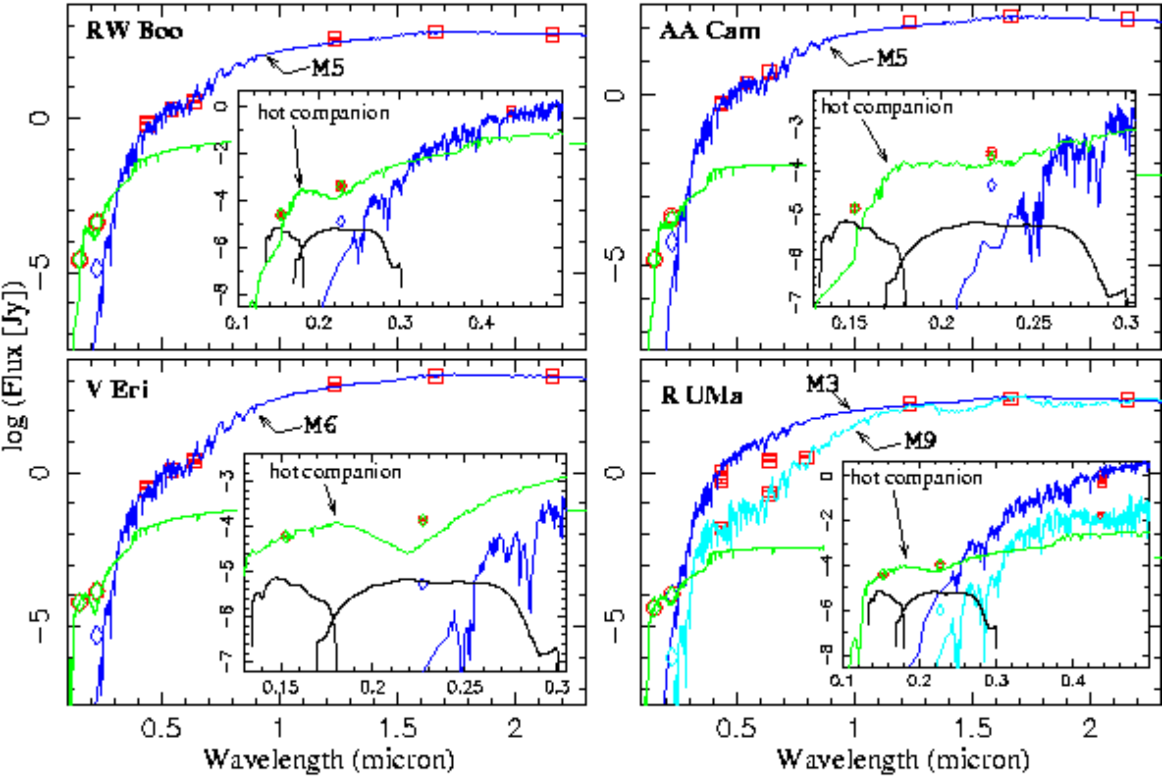

Indirect techniques such as radial-velocity (RV) or photospheric variability (PV) **NO GOOD**

UV observations!

cool primary (Teff < ~ 3000K), relatively low-luminosity main-sequence companion (Teff > ~ 6000K) detectable in

(blue/cyan curve: primary, green curve: companion, black curve: filter bandpass)

Sahai+2008; Ortiz & Guerrero 2016 carried out similar modeling for a larger sample and reached similar conclusions

FUV flux orders of magnitude above photospheric flux of AFB primary -- but variable!

=> Accretion activity associated with binary

Chromospheric emission? (*Montez et al. 2017*) -- probably not for FUV/NUV (>0.15)

FUV and NUV Properties of AGB Stars *(Sahai et al. 2019)*

Dominant fraction of UV-emitting AGB stars are NOT fuvAGB stars
Is it chromospheric emission? (*Montez et al. 2017***)**

- input catalog of ~3500 AGB stars, M4-M9, C-rich and S-stars

20% detected in one or both FUV and NUV bands
9% detected in both FUV and NUV bands
(above fractions likely lower limits because exposure times short, ~few x 100 s)

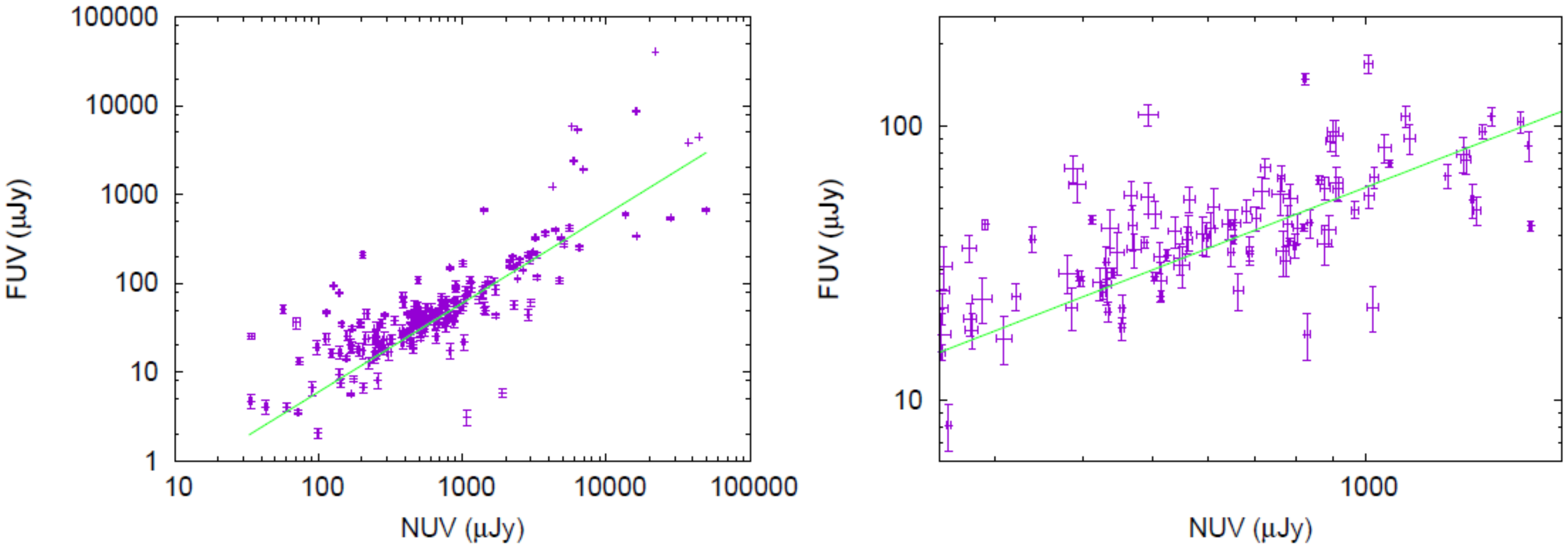

Mean FUV- and NUV-band GALEX fluxes of AGB stars
(sources detected in both UV bands with a signal-to-noise ratio, SNR >5)
green line: linear least-squares fit with outlier rejection, y = R(fuv/nuv) f(fuv),
R(uv/nuv)=0.06 (+/-0.002); expanded view of central region in right panel

FUV and NUV variability in fuvAGB stars

(Sahai, Sanchez Contreras & Sanz-Forcada 2016)

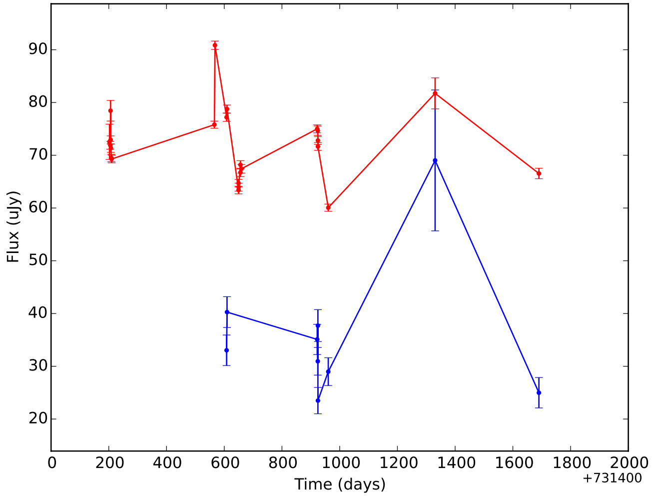

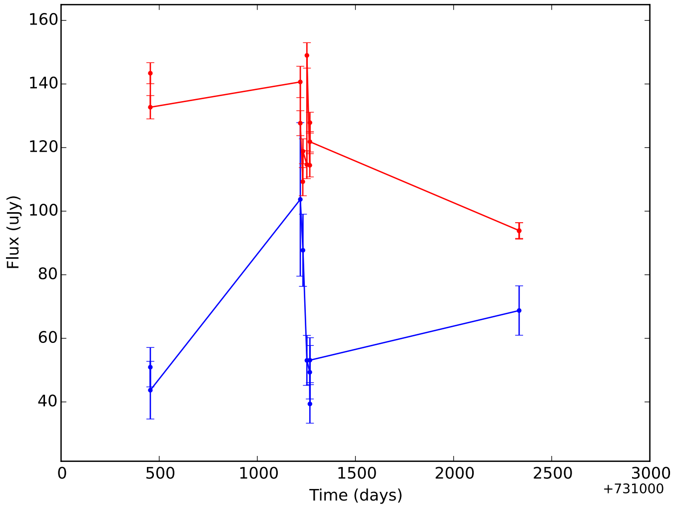

(FUV has been scaled up by factors 4-9)

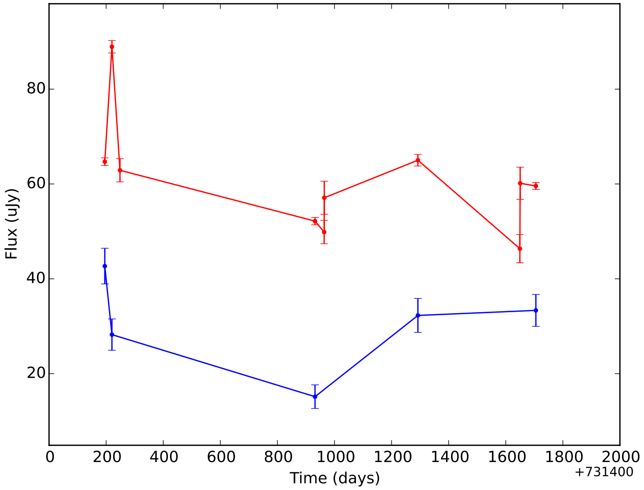

- Strong long-term (months-year) variability in both FUV and NUV

- We find
  (1) periods with FUV,NUV variations correlated (*variations in Emission Measure (EM)? obscuring column N_H?)*
  (2) periods with FUV,NUV variations anti-correlated (*variations in temperature, Tuv?)*

=> (variable) accretion-activity associated with binary companion

X-Ray Studies of fuvAGB Stars

(Ramstedt et al. 2012, Sahai et al. 2016, Ortiz & Guerrero 2021)

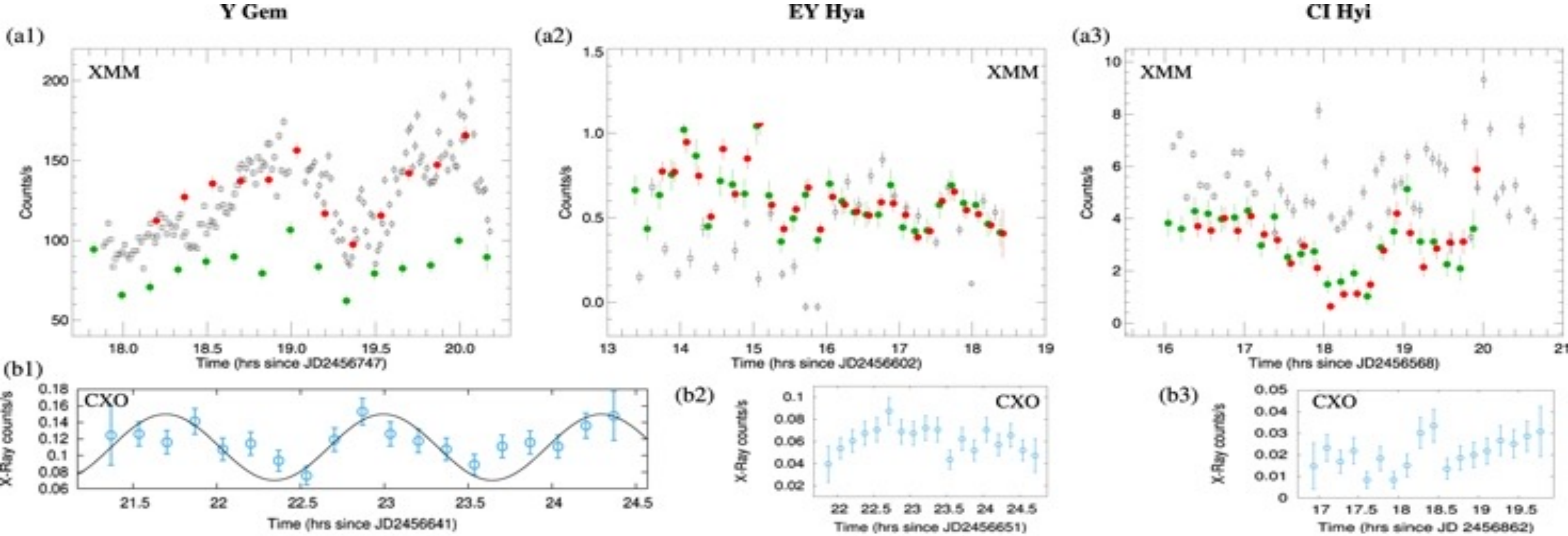

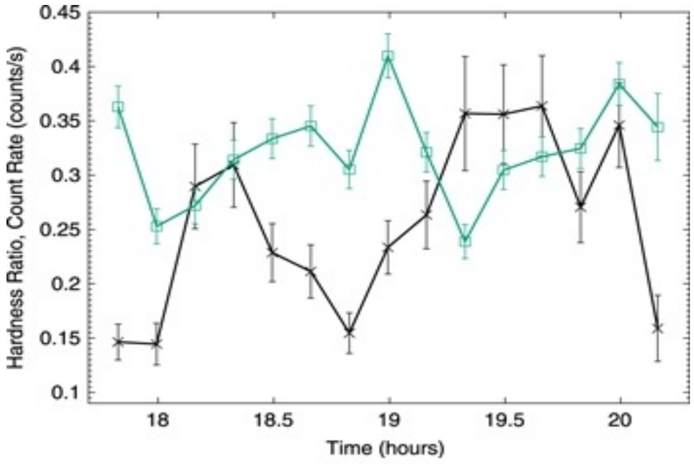

Sample of fuvAGB stars (stars with FUV emission), and R(fuv/nuv) > ~ 0.2; ~40% detected in Xrays)

- Quasi-periodic over hour-long timescale and stochastic variations (**flickering**)

Y Gem: hardness ratio (black curve) anti-correlated with flux (green curve)

- hence, unlikely to be flare activity
- most likely due to variations in NH (the obscuring neutral column density), perhaps due to changes in viewing geometry, and/or the presence of variable accretion streams

X-Ray Spectra of fuvAGB Stars *(Sahai et al. 2015)*

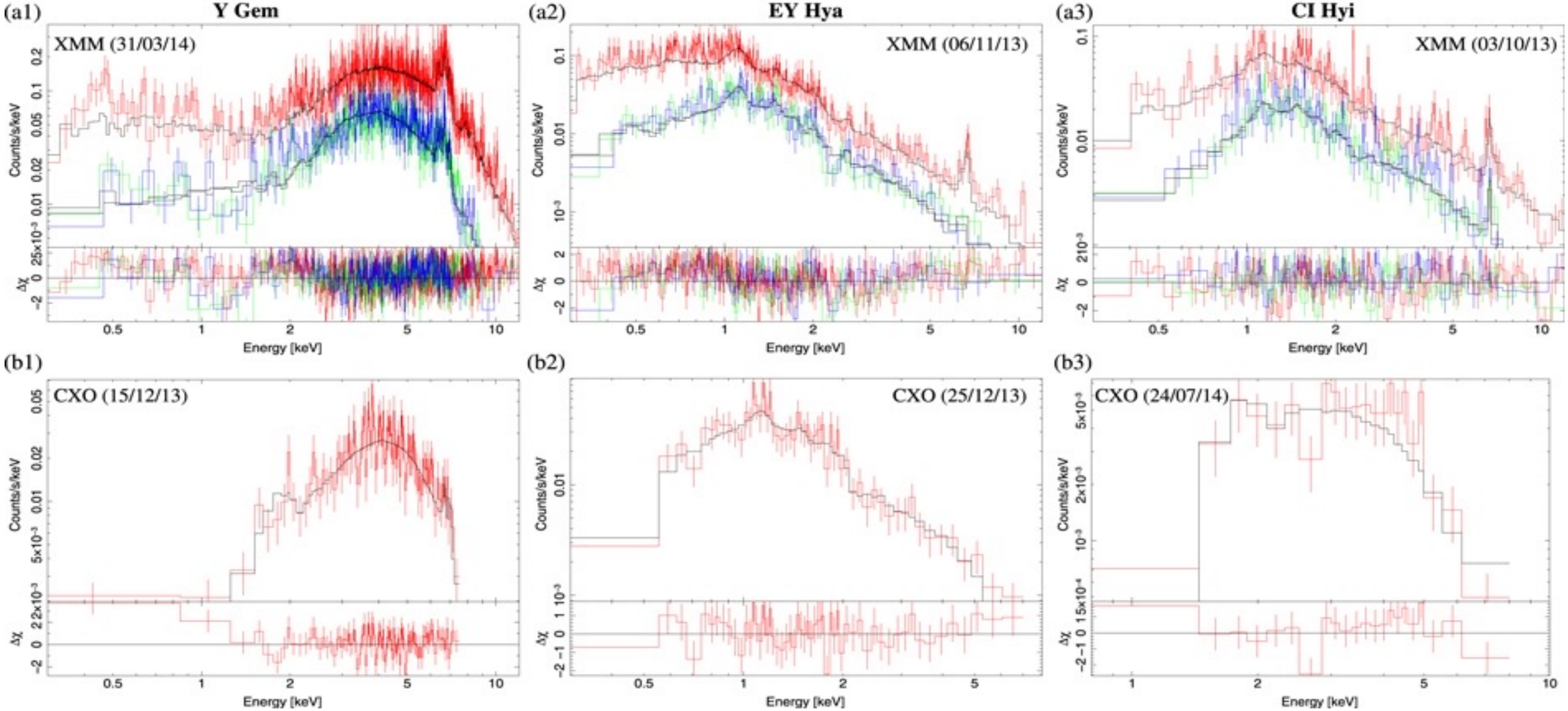

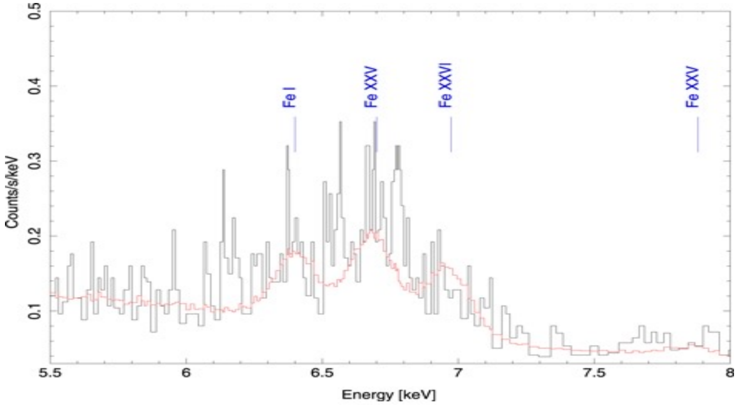

X-ray spectra fitted with APEC models

- X-ray temperature Tx (35-160 MK), Lx (0.002-0.2 Lsun), emission measure EM, column density of absorbing neutral column NH,
- Find coronal Fe lines (Fe xxv, xxvi: *all sources*) and neutral Fe line (*Y Gem, EY Hya?*)

=> **Accretion onto a disk around companion**

Flickering, High-Velocity Outflow and Infall (**Y Gem**)

(Sahai et al. 2018)

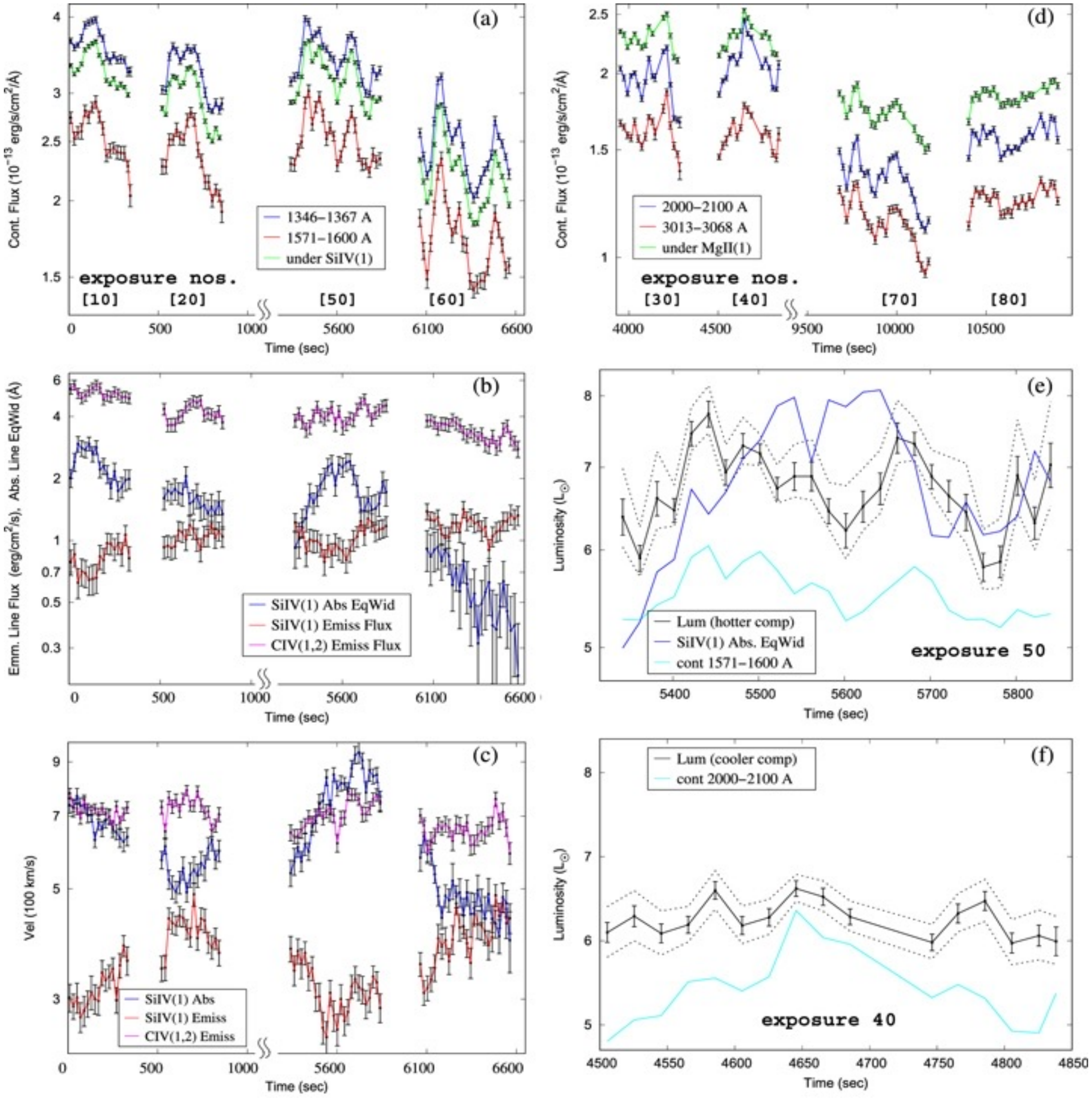

UV Flickering <~20 sec

(*optical flickering: Snaid+2018*)

=> Accretion Disk

Flux/Lum changes: **variations in accretion flow**

Emitting Region < ~0.1 AU

(size of accretion hot-spot?)

Continuum (blackbody fit)

$\Rightarrow L(accr) > 13\,L_\odot$

$< G\, dM/dt(accr)\, M_c / R_c$

$dM/dt(accr) > 5e\text{-}7\, M_\odot/yr$

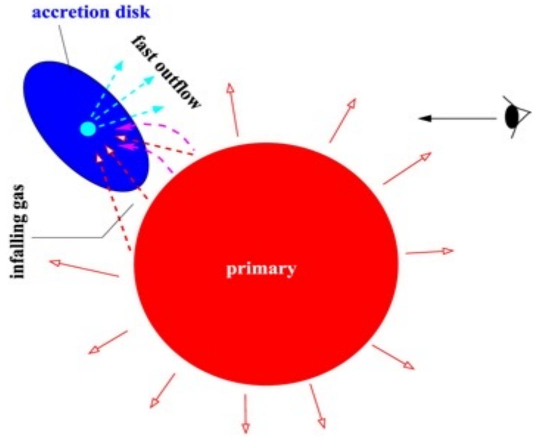

Roche-Lobe Overflow

Emission and absorption features, redshift/blueshift ~500 km/s

Modeling chromospheric emission (& constrain accretion-activity related emission)

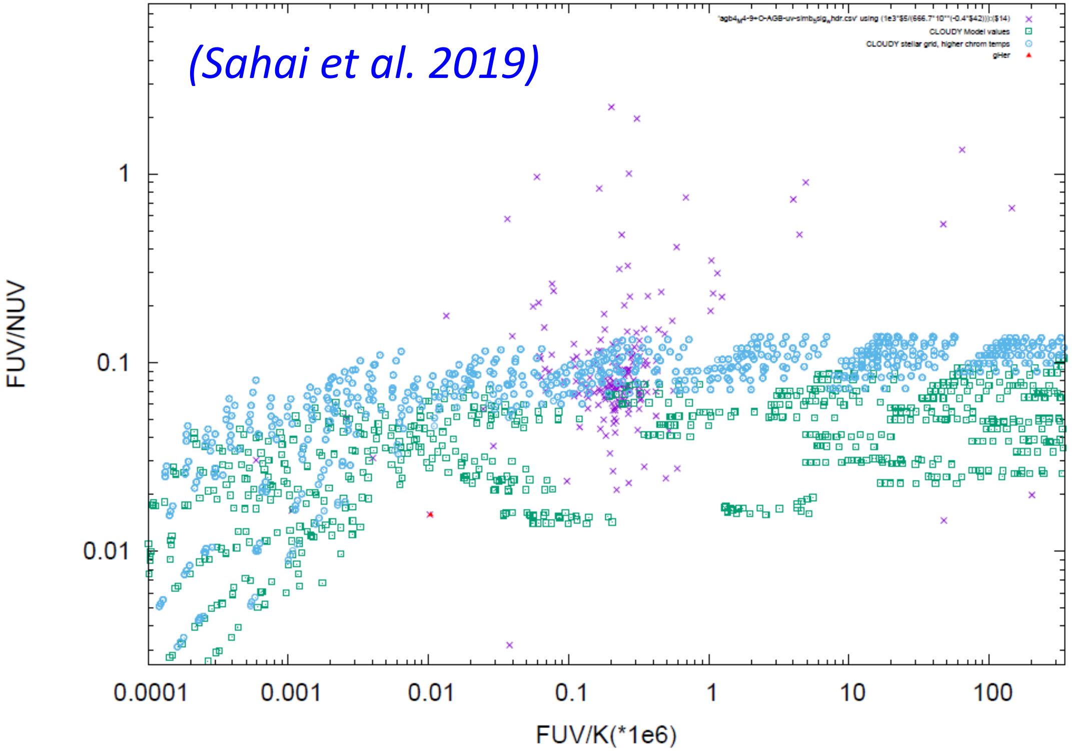

(Sahai et al. 2019)

(grid of ~50,000 CLOUDY models)

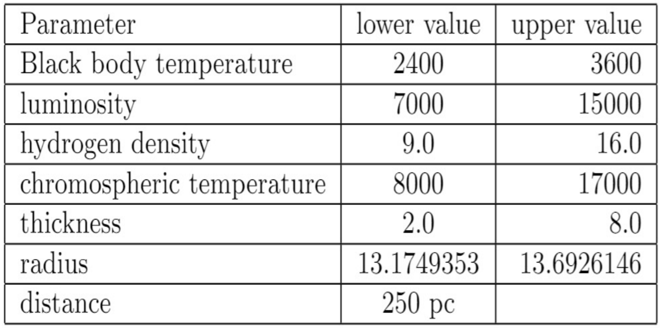

Parameter	lower value	upper value	
Black body temperature	2400	3600	
luminosity	7000	15000	
hydrogen density	9.0	16.0	log(cm^-3)
chromospheric temperature	8000	17000	
thickness	2.0	8.0	log(cm)
radius	13.1749353	13.6926146	log(cm)
distance	250 pc		

TABLE 2
MODEL PARAMETERS FOR FULL GRID OF CLOUDY MODELS

R(FUV/NUV) =0.06
T(chrom) ~ (9,000 -11,000)K

R(FUV/NUV)=0.06 to 0.1
T ~ (11,000 -15,000)K
too high for a chromosphere?

checks on our simple model: compare with

- MgII h & k line fluxes (IUE) of the AGB star gHer (*Luttermoser et al. 1994*)
- FUV-NUV STIS spectrum of Betelgeuse (*Carpenter et al. 2018*)

g Her chromosphere models

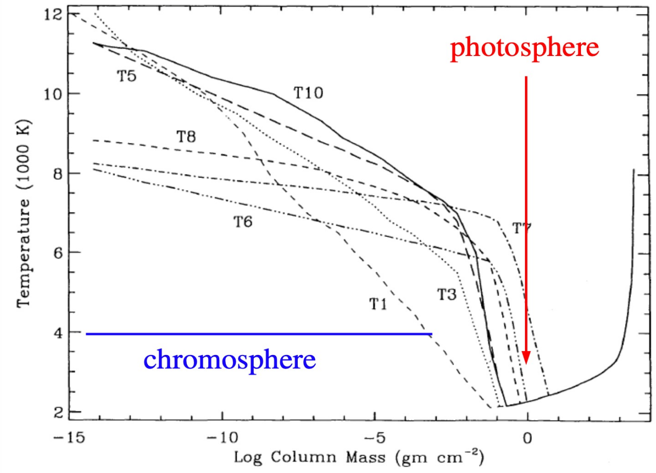

FIG. 2.—Temperature rises of representative chromospheric models. Temperature is displayed as a function of mass column density for models T1, T3, T5, T6, T7, T8, and T10. Note that model T10 is our final representative, one-dimensional chromosphere of g Her.

Summary

1) wide variety of morphologies during post-AGB phase (point-symmetry common)

2) PPNe/PNe: bipolar/multipolar shapes, low-latitude jets, nested geometrical structures

-- two classes of post-AGB objects (PPNe, dpAGB)

3) late-AGB / pAGB phase: highly-collimated jets (speeds ~few x 100 km/s, episodic, wobbling/ precessing) with very large scalar momenta (not radiatively driven)

4) dense torii, relatively large masses in PPNe, dpAGB (+ mm-size grains)

5) large (~100 AU), rotating disk(s) in dpAGB objects

6) A significant fraction of the galactic AGB star population show UV emission (> ~ 20% NUV, >~9 % NUV & FUV). UV emission is variable, indicative of variable accretion activity – presumably due to a binary companion – supported by detailed spectroscopic study of Y Gem, and X-ray studies of a small sample with high R(FUV/NUV))

For stars with R(FUV/NUV) > ~0.1, accretion activity likely mechanism for UV emission (supported by X-ray studies); for low R(FUV/NUV) <0.06, simple chromosphere models can produce the observed UV emission, but some fraction of these may also have companions

Binary interactions play a major role in the deaths of ordinary stars